Radical Ions

DOI: 10.1002/anie.201204106

A Triphenylamine Double-Decker: From a Delocalized Radical Cation to a Diradical Dication with an Excited Triplet State**

Yuichiro Yokoyama, Daisuke Sakamaki, Akihiro Ito, Kazuyoshi Tanaka, and Motoo Shiro*

Triphenylaminium radical cations are well-known for their remarkable stability; furthermore, the oxidation potential is adjustable by the introduction of a series of substituents, in particular, at the *para* positions. Thus, they are widely used not only as one-electron oxidative reagents but also as catalysts in organic chemistry.[1] Besides such an application as versatile chemical reagents, the ambient stable radical cations generated from triphenylamine (TPA) derivatives could be utilized as spin sources in molecule-based magnetic materials. In fact, a considerable number of TPA-based molecular multi-spin systems have appeared in the literature. However, from the viewpoint of assemblage of the spin sources into the architecture of the reported molecular systems, the spin–spin exchange coupling pathway has been confined to one- and two-dimensionalities,[2] and accordingly, TPA-based multispin systems with three-dimensional (3D) connectivity are rare.

In 1985, Neugebauer and co-workers reported the first synthesis of a TPA double-decker **1** (Scheme 1)[3] in which two TPA moieties are directly connected by threefold *o*,*o*′-linkage, in association with an interest in intramolecular interaction between two nitrogen lone pairs.[4] In spite of its sensitivity to oxidation and the formation of persistent radical cation, no detailed information was available concerning the electronic structure. Such a cage-like oligo(triphenylamine) can be regarded as a potent building block to afford the opportunity furnishing new TPA-based macromolecular systems with genuine 3D connectivity. Although neither the parent **1** nor its derivatives have been reported since then,[5] an analogue **2** in which two TPA moieties are connected at *para* positions of all phenyl groups by three *meta*-phenylenediamine pillars, was successfully prepared in our laboratory.

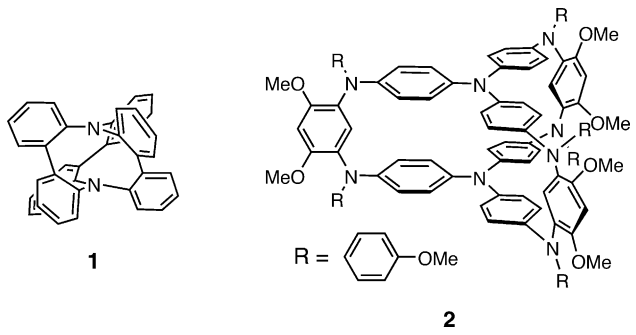

Scheme 1. The first reported TPA double-decker **1**[3] and *meta*-phenylenediamine-bridged TPA double-decker **2**.

Slow evaporation of a dilute mixed solution (CH_3OH and CH_2Cl_2) of a pale yellow product **2**, which was obtained by using Buchwald–Hartwig cross-coupling reaction[6] between 4,4′,4″-tribromo-TPA as a deck and *meta*-phenylenediamine as a pillar in a ratio of 2:3,[7] gave yellow block crystals suitable for X-ray structure analysis.[21] The crystal belongs to the space group $P2_1$, and contains two molecules of **2** per unit cell in which there exist three sites for CH_2Cl_2 molecules so as to fill spaces between the double-deckers (Supporting Information, Table S1).

The X-ray structure of **2** has almost C_{3h} symmetrical trichetria-like[8] shape when all the methoxy substituents are ignored, and the upper and lower TPA decks adopt almost planar propeller-like conformation (the tilted angles of phenyl rings range from 42° to 53°), and moreover, are totally eclipsed (Figure 1). Three *meta*-phenylenediamine planes are perpendicular to the TPA planes, and therefore, the distance between two TPA decks are estimated to be about 4.9 Å at the peripheral three nitrogen pairs and 5.8 Å at the central nitrogen pair, indicating the direct transannular π–π interaction between two TPA decks is virtually ignorable. The sp^2 planes of the nitrogen atoms in the *meta*-phenylenediamine as a pillar are found to be at angles of about 60° to the *meta*-phenylene plane.

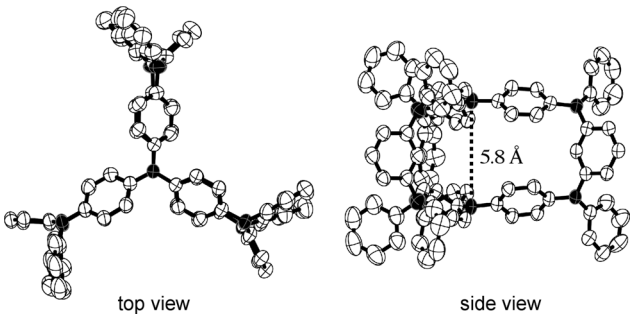

Figure 1. Two ORTEP views of **2**. Ellipsoids are set at 50% probability; solvent molecules of crystallization, methoxy groups, and hydrogen atoms are omitted for clarity. Nitrogen atoms are colored in black.

[*] Y. Yokoyama, D. Sakamaki, Dr. A. Ito, Prof. Dr. K. Tanaka
Department of Molecular Engineering
Graduate School of Engineering, Kyoto University
Nishikyo-ku, Kyoto 615-8510 (Japan)
E-mail: aito@scl.kyoto-u.ac.jp
Dr. M. Shiro
Rigaku Corporation, X-ray Research Laboratory
Matsubaracho 3-9-12, Akishima, Tokyo, 196-8666 (Japan)

[**] The present work was supported by Grant-in-Aid for Scientific Research (B) (20350065) from the Japan Society for the Promotion of Science (JSPS). D.S. thanks the JSPS Research Fellowship for Young Scientists.

Supporting information for this article is available on the WWW under http://dx.doi.org/10.1002/anie.201204106.

In accordance with the X-ray structure, DFT calculations (B3LYP/6-31G* level of theory) also demonstrated that the C_{3h}-symmetric structure was adopted for a model compound **2′** in which all the methoxy groups are replaced by hydrogen atoms. As is apparent from the HOMO (Figure 2a), the spin

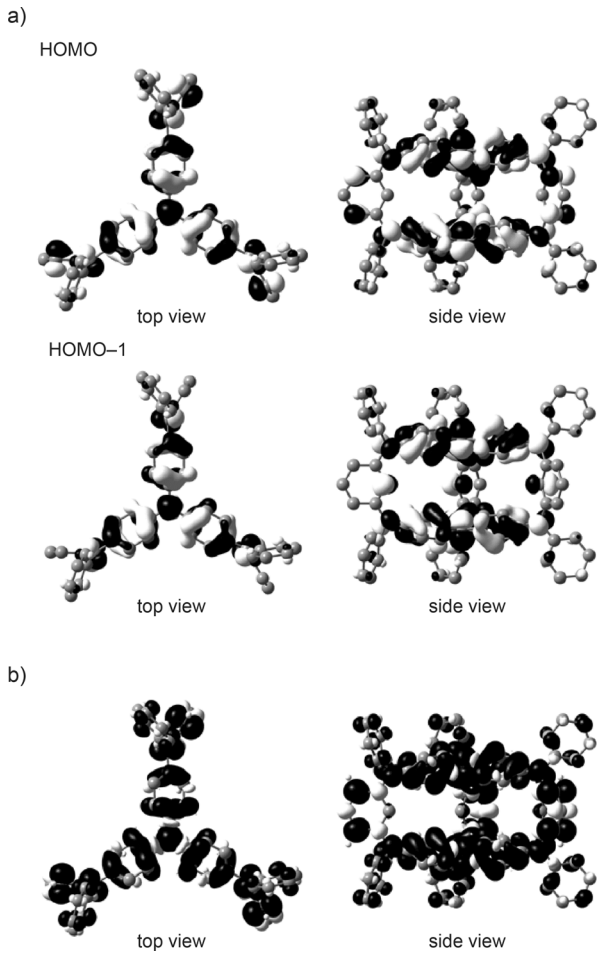

Figure 2. a) HOMO and HOMO−1 (B3LYP/6-31G*) of **2′**; b) spin-density distribution of $\mathbf{2'}^{+}$ (black: positive spin, white: negative spin; spin isosurface value = 0.0003 electron au^{-3}).

density distribution in $\mathbf{2'}^{+}$ revealed delocalization over the entire molecule (Figure 2b). Although the C_{3h} symmetric structure is retained on going from **2′** to $\mathbf{2'}^{4+}$, the quinoid-type deformation in TPA decks was predicted to be remarkable with increase in the degree of oxidation (Supporting Information, Table S2).

Double-decker **2** exhibited multiple redox behavior owing to contribution from the eight TPA redox centers. The observed five oxidation waves are chemically reversible, and the oxidation potentials [E_{ox}^{n} vs. $Fc^{0/+}$ (*n*e)] are determined to be $E_{ox}^{1} = -0.33$ V (1e), $E_{ox}^{2} = -0.16$ V (1e), $E_{ox}^{3} = +0.09$ V (2e), $E_{ox}^{4} = +0.46$ V (1e), and $E_{ox}^{5} = +0.61$ V (1e) on the basis of cyclic voltammetry (CV) and differential pulse voltammetry (DPV) (Figure 3). It should be noted that although *meta*-phenylene linkage is included in connectivity of **2**, the first oxidation potential of $E_{ox}^{1} = -0.33$ V is more negative than that of the related all-*para*-phenylene-linked TPA oligomers:

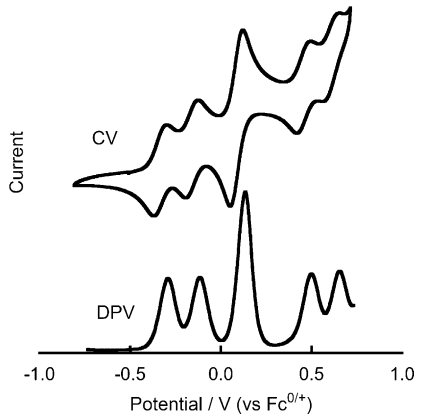

Figure 3. Cyclic voltammogram (CV) and differential pulse voltammogram (DPV) of **2**, measured in CH_2Cl_2 containing 0.1 M nBu_4NBF_4 at 298 K (scan rate 100 mV s^{-1}).

hexaaza[1$_6$]paracyclophane ($E_{ox}^{1} = -0.28$ V)[9] and the second generation of dendritic triphenylamines ($E_{ox}^{1} = -0.30$ V).[10] Taking this into account, **2** is considered to be a good electron donor, and indeed it afforded the charge-transfer (CT) complex with 7,7,8,8-tetracyano-*p*-quinodimethane (TCNQ) in the ratio of 1:1 (Supporting Information, Figure S3). More interestingly, the splitting of redox potentials ($E_{ox}^{2} - E_{ox}^{1} = 170$ mV) indicates a relatively strong electronic coupling between two TPA decks, irrespective of *meta*-phenylene linkage, and therefore, the intervalence state between the two redox-active TPA decks is expected to appear in radical cation of **2**, as has been elaborately been investigated for TPA-based organic mixed-valence compounds.[11] This is also supported by comparison with the first oxidation potential ($E_{ox}^{1} = -0.16$ V (1e)) for the reference compound **3**[10] corresponding to a single TPA deck (Scheme 2). Furthermore, two charged radical centers generated by the second oxidation process of **2** are located separately on the upper and lower TPA decks to alleviate the energetically unfavorable Coulombic repulsion, and as a consequence, magnetic interaction takes place between the two-spin system.

On the basis of the electrochemical studies, we measured the optical absorption spectral change of double-decker **2** in CH_2Cl_2 during the course of the oxidation going from neutral to tetracation $\mathbf{2}^{4+}$ by using optically transparent thin-layer electrochemical cell (Supporting Information, Figure S4). To

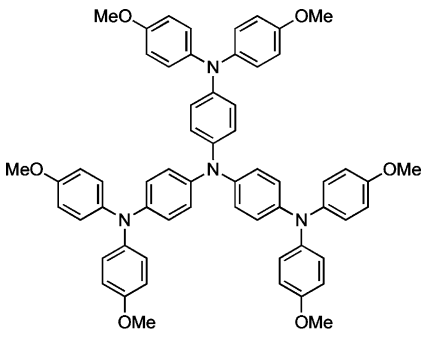

3

Scheme 2. Reference compound **3** for a single TPA deck.

gain insights into the charge distribution of the oxidized double-decker, only the spectral change in the lowest energy transitions of $\mathbf{2}^{+}$ to $\mathbf{2}^{4+}$ will be discussed (Figure 4). The lowest

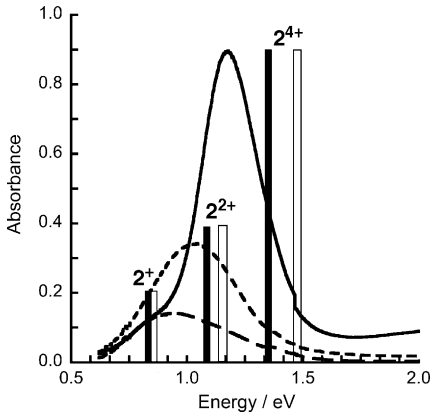

Figure 4. Vis-NIR absorption spectra of the stepwise electrochemical oxidation of **2** to tetracation $\mathbf{2}^{4+}$ in CH_2Cl_2/0.1 M nBu_4NBF_4 at 298 K. ----- $\mathbf{2}^{+}$, •••• $\mathbf{2}^{2+}$, —— $\mathbf{2}^{4+}$. The black and white sticks designate the TD-DFT-calculated lowest-energy transition energies and their relative oscillator strengths for $\mathbf{2'}^{+}$, $\mathbf{2'}^{2+}$, and $\mathbf{2'}^{4+}$ at B3LYP/6-31G* and B1LYP-(a=0.35)/SVP with CPCM solvent model for CH_2Cl_2.

energy band at 1332 nm (0.93 eV) observed for $\mathbf{2}^{+}$ is blue-shifted to 1190 nm (1.04 eV) when oxidized into $\mathbf{2}^{2+}$, and the shifted band becomes twice as intense as that for $\mathbf{2}^{+}$. Further oxidation to $\mathbf{2}^{4+}$ resulted in a far more intense band with a further blue-shift (1053 nm (1.18 eV)).[12] For comparison, the spectroelectrochemical measurements were also performed for the reference compound **3** (Supporting Information, Figure S5).[12] As a consequence, the observed spectrum for $\mathbf{3}^{+}$ was found to be in good accordance with that for $\mathbf{2}^{2+}$. This result strongly suggests that two charged radical centers in $\mathbf{2}^{2+}$ are located separately on the upper and lower TPA decks. Furthermore, both spectra observed for $\mathbf{2}^{4+}$ and $\mathbf{3}^{2+}$ were obviously similar, although the maximum wavelength for the lowest energy band for $\mathbf{2}^{2+}$ remained unchanged (1190 nm (1.04 eV)). Excitation energies for the oxidized species, $\mathbf{2'}^{+}$, $\mathbf{2'}^{2+}$, and $\mathbf{2'}^{4+}$, were estimated by the time-dependent DFT (TD-DFT) calculations[13] (Supporting Information, Figure S2 and Table S3). As shown in Figure 4, the characteristics of the observed spectral change is reasonably reproduced by the theoretical results for the model compound $\mathbf{2'}$. Recently, Kaupp and co-workers pointed out the fact that the frequently used B3LYP hybrid functional may lead to erroneous results in organic mixed-valence compounds.[14] Thus, in addition to the B3LYP calculations, we have also performed the DFT optimizations and TD-DFT calculations for $\mathbf{2'}^{+}$, $\mathbf{2'}^{2+}$, and $\mathbf{2'}^{4+}$ by using the B1LYP hybrid functional with 35% exact exchange and the SVP basis sets,[15] as has been recommended by Kaupp and co-workers.[14] Furthermore, solvents effects have been included by the CPCM polarizable conductor calculation model for CH_2Cl_2 (ε = 8.93).[16] These calculations resulted in the same trend as B3LYP ones, although the transition energies showed small blue-shifts (Figure 4; Supporting Information, Table S4). Therefore, the present TD-DFT calculations strongly suggest that the charged species of $\mathbf{2}^{+}$ to $\mathbf{2}^{4+}$ are in delocalized intervalence states. In particular, the lowest-energy band for $\mathbf{2}^{+}$ is assignable to a transition from doubly degenerate β ((HO-1)MOs) to β (LUMO), which corresponds to the charge resonance between the *meta*-phenylenediamine moieties as pillars and the core TPA decks. Moreover, the intervalence band observed for $\mathbf{2}^{+}$ exhibited no noticeable solvatochromism in CH_2Cl_2 (ε = 8.93) and benzonitrile (ε = 25.59), thus supporting a charge-delocalized character for $\mathbf{2}^{+}$ (Supporting Information, Figure S7).

Treatment of **2** with 1 equiv of tris(4-bromophenyl)aminium hexachloroantimonate (Magic Blue)[1c] in CH_2Cl_2 at 195 K gave a green solution for $\mathbf{2}^{+}$. However, the solution ESR spectrum showed a single broad line with no hyperfine structures (g = 2.0024; ΔH_{pp} (peak-to-peak linewidth) = 1.05 mT), thus affording no information on the spin distribution over the molecular skeleton (Supporting Information, Figure S8). On the other hand, the evidence of a diradical dication for the oxidized species treated by two equiv of the Magic Blue was confirmed by the fine-structured ESR spectrum characteristic for spin-triplet species in the $g \approx 2$ region, as well as by the weak signal corresponding to the forbidden transition in the $g \approx 4$ region (Figure 5). From the

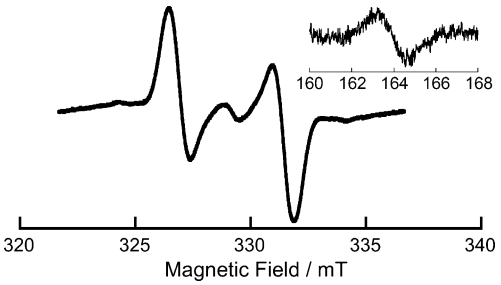

Figure 5. ESR spectrum of $\mathbf{2}^{2+}$ in CH_2Cl_2/*n*-butyronitrile (3:1) at 123 K. Inset: forbidden resonance observed at 123 K.

zero-field splitting parameters (D = 4.9 mT and $E \cong 0$ mT), the average distance between the radical centers[17] was estimated to be 8.3 Å. The deviation from the face-to-face distance between the two TPA decks (5.8 Å) determined by X-ray analysis strongly suggests that spin-density distributions on each TPA decks are to some extent delocalized over *meta*-phenylenediamine pillars. Figure 6 displays the temperature dependence of the ESR signal intensity for $\mathbf{2}^{2+}$, and the ground state of $\mathbf{2}^{2+}$ turned out to be in spin-singlet state, apparently from decrease in intensity with decreasing temperature. The energy gap between the singlet and triplet states ($\Delta E_{S\text{-}T}$) was estimated to be -0.18 kcal mol^{-1} as a result of curve-fitting with the Bleaney–Bowers singlet–triplet model equation [Eq. (1)].[18]

$$I = \frac{C}{T}\frac{1}{3 + \exp\left(-\frac{\Delta E_{S\text{-}T}}{k_B T}\right)} \quad (1)$$

On the other hand, as shown in Figure 2a (see also the Supporting Information, Figure S1), the HOMO and HOMO−1 of $\mathbf{2'}$ were found to be of the nondisjoint (or

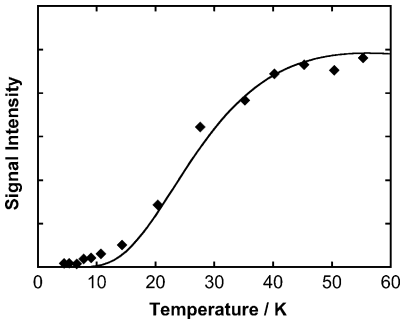

Figure 6. Temperature dependence of the ESR signal intensity of $\mathbf{2}^{2+}$ and the curve-fitting (solid line) with the Bleaney–Bowers singlet–triplet model equation (see text).

coextensive) nonbonding type (NBMOs),[19] which is reflected in the orbital patterns over *meta*-phenylenediamine moieties, and moreover, the quasi degeneracy and nondisjoint character suggested the high-spin preference for $\mathbf{2}'^{2+}$ ($\Delta E_{S-T} = 5.3$ kcal mol^{-1}). The discrepancy between the DFT-calculated energy gap and the experimental result can be ascribed to the fact that the static correlation, in particular, for the singlet state of $\mathbf{2}^{2+}$ is inadequately taken into consideration in the present DFT calculations, and therefore, the present calculations failed to attest the significant effect that large dihedral angle (60° to 90°) between *meta*-phenylene π-plane and the spin-bearing groups results in the preference of a spin-singlet ground state in diradicals.[20] In contrast, tetracation $\mathbf{2}^{4+}$, generated by treatment of **2** with four equiv of the Magic Blue, was ESR silent (Supporting Information, Figure S9), in good accordance with the theoretical consideration.

In conclusion, we have described the electronic structures for the polycationic states of a double-layered TPA linked by three *meta*-phenylenediamine pillars, that is, TPA double-decker. As exemplified by the X-ray analysis, no direct through-space interaction between two nitrogen lone pairs on both TPA decks can be inferred. However, it was clarified that the generated spin in $\mathbf{2}^{+}$ is delocalized over the whole molecular skeleton, which is probably due to through-bond interaction through three-dimensional connectivity in **2**. Furthermore, although the dication of **2** revealed the diradical character originating from the nondisjoint quasi doubly degenerate NBMOs owing to three *meta*-phenylenediamine pillars, its spin preference was contrary to the simple B3LYP prediction. The outcome of the present study demonstrates that it is not straightforward to endow three-dimensionally connected TPA-based macromolecular systems with desired electronic properties. To put it the other way around, however, intriguing electronic features can be emerged from this class of molecular systems. The extension to multiple-deckers and the construction of the other related TPA-based architectures with complicated connectivity are currently underway in our laboratory.

Received: May 26, 2012
Revised: July 10, 2012
Published online: August 21, 2012

Keywords: arylamines · cyclophanes · electrochemistry · EPR spectroscopy · radical ions

[1] a) F. A. Bell, A. Ledwith, D. C. Sherrington, *J. Chem. Soc.* **1969**, 2719; b) S. Dapperheld, E. Steckhan, K.-H. Grosse Brinkhaus, T. Esch, *Chem. Ber.* **1991**, *124*, 2557; c) N. G. Connelly, W. E. Geiger, *Chem. Rev.* **1996**, *96*, 877.
[2] For example, see: a) X. Z. Yan, J. Pawlas, T. Goodson III, J. F. Hartwig, *J. Am. Chem. Soc.* **2005**, *127*, 9105; b) A. Ito, Y. Yamagishi, K. Fukui, S. Inoue, Y. Hirao, K. Furukawa, T. Kato, K. Tanaka, *Chem. Commun.* **2008**, 6573.
[3] F. A. Neugebauer, S. Kuhnhäuser, *Angew. Chem.* **1985**, *97*, 589; *Angew. Chem. Int. Ed. Engl.* **1985**, *24*, 596.
[4] R. W. Alder, S. P. East, *Chem. Rev.* **1996**, *96*, 2097.
[5] For closely related caged compounds, see: a) D. O'Krongly, S. R. Denmeade, M. Y. Chiang, R. Breslow, *J. Am. Chem. Soc.* **1985**, *107*, 5544; b) B. P. Friedrichsen, H. W. Whitlock, *J. Am. Chem. Soc.* **1989**, *111*, 9132; c) B. P. Friedrichsen, D. R. Powell, H. W. Whitlock, *J. Am. Chem. Soc.* **1990**, *112*, 8931; d) R. Berscheid, M. Nieger, F. Vögtle, *Chem. Ber.* **1992**, *125*, 1687; e) F. Vögtle, J. Winkel, *Tetrahedron Lett.* **1979**, *20*, 1561; f) H. Schrage, J. Franke, F. Vögtle, E. Steckhan, *Angew. Chem.* **1986**, *98*, 335; *Angew. Chem. Int. Ed. Engl.* **1986**, *25*, 336; g) F. Vögtle, G. Hohner, *Top. Curr. Chem.* **1978**, *74*, 1.
[6] a) J. P. Wolfe, S. Wagaw, J. F. Marcoux, S. L. Buchwald, *Acc. Chem. Res.* **1998**, *31*, 805; b) J. F. Hartwig, *Acc. Chem. Res.* **1998**, *31*, 852; c) J. F. Hartwig, *Angew. Chem.* **1998**, *110*, 2154; *Angew. Chem. Int. Ed.* **1998**, *37*, 2046; d) A. R. Muci, S. L. Buchwald, *Top. Curr. Chem.* **2002**, *219*, 133.
[7] Synthetic procedures for **2** are described in the Supporting Information.
[8] P. A. Ashton, N. S. Isaacs, F. H. Kohnke, G. S. D'Alcontres, J. F. Stoddart, *Angew. Chem.* **1989**, *101*, 1269; *Angew. Chem. Int. Ed. Engl.* **1989**, *28*, 1261.
[9] A. Ito, Y. Yokoyama, R. Aihara, K. Fukui, S. Eguchi, K. Shizu, T. Sato, K. Tanaka, *Angew. Chem.* **2010**, *122*, 8381; *Angew. Chem. Int. Ed.* **2010**, *49*, 8205.
[10] A. Ito, D. Sakamaki, Y. Ichikawa, K. Tanaka, *Chem. Mater.* **2011**, *23*, 841.
[11] a) J. Hankache, O. S. Wenger, *Chem. Rev.* **2011**, *111*, 5138; b) A. Heckmann, C. Lambert, *Angew. Chem.* **2012**, *124*, 334; *Angew. Chem. Int. Ed.* **2012**, *51*, 326, and references therein.
[12] Oxidation states higher than $\mathbf{2}^{4+}$ and $\mathbf{3}^{2+}$ were found to be unstable under the experimental conditions in the present spectroelectrochemical study.
[13] a) R. Bauernschmitt, R. Ahlrichs, *Chem. Phys. Lett.* **1996**, *256*, 454; b) M. E. Casida, C. Jamorski, K. C. Casida, D. R. Salahub, *J. Chem. Phys.* **1998**, *108*, 4439; c) R. E. Stratmann, G. E. Scuseria, M. J. Frisch, *J. Chem. Phys.* **1998**, *109*, 8218.
[14] M. Renz, K. Theilacker, C. Lambert, M. Kaupp, *J. Am. Chem. Soc.* **2009**, *131*, 16292.
[15] A. Schäfer, H. Horn, R. Ahlrichs, *J. Chem. Phys.* **1992**, *97*, 2571.
[16] V. Barone, M. Cossi, *J. Phys. Chem. A* **1998**, *102*, 1995.
[17] W. B. Gleason, R. E. Barnett, *J. Am. Chem. Soc.* **1976**, *98*, 2701.
[18] B. Bleaney, K. D. Bowers, *Proc. R. Soc. London Ser. A* **1952**, *214*, 451.
[19] a) D. A. Dougherty, *Acc. Chem. Res.* **1991**, *24*, 88; b) J. A. Crayston, J. N. Devine, J. C. Walton, *Tetrahedron* **2000**, *56*, 7829.
[20] a) F. Kanno, K. Inoue, K. Noboru, H. Iwamura, *J. Am. Chem. Soc.* **1993**, *115*, 847; b) S. Fang, M.-S. Lee, D. A. Hrovat, W. T. Borden, *J. Am. Chem. Soc.* **1995**, *117*, 6727.
[21] CCDC 879827 (**2**) contains the supplementary crystallographic data for this paper. These data can be obtained free of charge from The Cambridge Crystallographic Data Centre via www.ccdc.cam.ac.uk/data_request/cif.

